Catena 83 (2010) 107–118

Contents lists available at ScienceDirect

Catena

journal homepage: www.elsevier.com/locate/catena

Spatio-temporal reconstruction of snow avalanche activity using tree rings: Pierres Jean Jeanne avalanche talus, Massif de l'Oisans, France

Corona Christophe [a,*], Rovéra Georges [b], Lopez Saez Jérôme [a], Stoffel Markus [c,d], Perfettini Pascal [e]

[a] Cemagref UR EMGR, 2 rue de la papeterie, BP 76 F-38402 Saint-Martin d'Hères Cedex, France
[b] Institut de Géographie Alpine, Laboratoire Politiques publiques, Action Politique, Territoires (PACTE) UMR 5194 du CNRS, Université Joseph Fourier, 14 bis avenue Marie Reynoard, 38100 Grenoble, France
[c] Laboratory of Dendrogeomorphology (dendrolab.ch), Institute of Geological Sciences, University of Bern, Baltzerstrasse 1+3, 3012 Bern, Switzerland
[d] Institute for Environmental Sciences (ISE), University of Geneva, route de Drize 7, 1227 Carouge-Geneva, Switzerland
[e] Cemagref de Grenoble, Unité Erosion Torrentielle Neige et Avalanche, Domaine Universitaire, 2 rue de la papeterie BP 76, 38402 Saint-Martin d'Hères, France

ARTICLE INFO

Article history:
Received 22 September 2009
Received in revised form 29 July 2010
Accepted 6 August 2010

Keywords:
Dendrogeomorphology
Growth disturbances
Snow avalanches
Frequency
Spatial analysis
French Alps

ABSTRACT

Snow avalanches are a major threat in many parts of the Alps, where they periodically damage infrastructure, disrupt transportation corridors or even cause loss of life. Nonetheless, the spatial behavior of past avalanche activity and the analysis of areas affected during particular events remain often imprecise. It was therefore the purpose of this study to reconstruct spatio-temporal patterns of past avalanche activity on a forested avalanche talus in the French Alps (Pierres Jean Jeanne talus, Massif de l'Oisans, France). A total of 232 European larches (*Larix decidua* Mill.) with clear signs of snow wasting events was analyzed and growth disturbances (GD) related to avalanche activity was assessed, such as tangential rows of traumatic resin ducts, the onset of compression wood or abrupt growth suppression and release. In total, 901 GD were identified in the tree-ring samples, indicating that 20 high-magnitude avalanches occurred between AD 1919 and 1994. The mean return period of snow avalanches was ~4 years with a ~26% probability that an avalanche occurs in any particular year. Interpolated maps allowed for explicit spatial estimates of return periods throughout the talus, showing a rapid increase of return frequency from 2.5 to 50 years with increasing distance from the talus apex. The distribution of avalanche years seems to be quite homogeneous in time with a gap between 1951 and 1959 and since 1994. Snowfall from a nearby meteorological station (Saint-Christophe en Oisans; 10 km from the study site) indicated that the five most recent high-magnitude events on record occurred due to above-average snowfall anomalies in December and January associated with abnormally low air temperatures. Findings suggest that a strong snow metamorphism under high temperature gradients in January could explain the occurrence of high-magnitude snow avalanches.

1. Introduction

Like other disturbances, snow avalanches vary in kind, frequency, magnitude, intensity and severity (McClung and Schaerer, 1993). They result from interactions between climatic factors, local topography and the existing snow pack structure (Hebertson and Jenkins, 2003). In mountain areas, like the Alps, snow avalanches pose a hazard to human activities (Mears, 1992), they endanger settlements and may cause heavy damage to infrastructure or transportation routes. In France, snow avalanches are causing thirty deaths every year (Ancey, 1998). Avalanche risk has increased as a result of diversified human activities (Jomelli et al., 2007) and through the recent colonization of numerous avalanche paths with vegetation, thus masking potentially dangerous avalanche flow paths (Didier and Brun, 1998; Corona, 2007). An accurate database on return periods of avalanches, their spatial extent and on factors contributing to their triggering is therefore essential for land-use planning and management (Gruber and Margreth, 2001).

The best means of estimating the return period and magnitude of snow avalanches is the study of historical sources and the monitoring of avalanche paths (Glass et al., 2000). Numerous avalanche chronicles spanning several decades or centuries exist near settlements in the Alps (Casteller et al., 2007), but most often only catastrophic events are accurately documented due to the fact that they remain in collective memory for a long time (Decaulne and Saemundsson, 2006). Additionally, in France, public historical records are available from the Standing Investigation of Avalanche Survey (Enquête Permanente des Avalanches; hereafter referred to as EPA) which was initiated by foresters in the early 1900s (Jomelli et al., 2007). Approximately 4400 sites throughout the French Alps and the French Pyrenees are systematically monitored for variable periods up to a century, due to their potential threat to existing or projected

* Corresponding author.
E-mail addresses: christophe.corona@cemagref.fr (C. Christophe), georges.rovera@ujf-grenoble.fr (R. Georges), jerome.lopez@cemagref.fr (L.S. Jérôme), markus.stoffel@dendrolab.ch (S. Markus).

0341-8162/$ – see front matter © 2010 Elsevier B.V. All rights reserved.
doi:10.1016/j.catena.2010.08.004

infrastructure and for their ease of observation (Jamard and Garcia, 2002). These EPA are usually complemented with a map localizing the occurrence of avalanches (Carte de Localisation des Phénomènes Avalancheux; hereafter referred to as CLPA), but these maps usually cover only a limited time span with frequent omission of events.

In the French Alps, an almost systematic lack of data has also limited investigations focusing on factors contributing to major avalanches in remote areas of the French Alps. Studies have either examined one event that occurred during an exceptional season (Allix, 1923; Navarre et al., 1991; Villecrose, 2001) or focused on avalanche activity in relation to climate using physical models developed by Météo France (e.g., SAFRAN-MEPRA-CROCUS; Durand et al., 1999). In contrast, only a very limited number of studies (Jomelli et al., 2007) have attempted to understand factors associated with avalanche events that occurred within a given path over a relatively long period of the past.

In wooded avalanche paths, the use of tree rings may greatly help documentation of past events and may allow reconstruction of precise chronologies of major avalanche activity over considerable periods of the past. Early dendrogeomorphic studies of snow avalanches date back to the late 1960s and the method has been used extensively in the United States (e.g. Potter, 1969; Carrara, 1979; Butler and Malanson, 1985; Rayback, 1998; Reardon et al., 2008) and in Canada (e.g. Schaerer, 1972; Frazer, 1985; Dubé et al., 2004) ever since. For further details on North American snow avalanche research, Butler and Sawyer (2008) provide a recent overview. In Europe, tree-ring analyses have been conducted to reconstruct the frequency and extent of avalanches in Scotland (Ward, 1985), the Spanish Pyrenees (Muntan et al., 2004; Muntan et al., 2009), the Italian (Comunello et al., 2001; Bezzi et al., 2003) and Swiss Alps (Stoffel et al., 2006; Casteller et al., 2007). To date, chronologies of avalanching based on proxy data with a one-year resolution do not exist for the French Alps.

The purpose of this study therefore was to provide (i) a high-resolution chronology of high-magnitude events for an avalanche talus slope located in the Romanche Valley in the Oisans Massif (French Alps) using dendrogeomorphic methods. This tree-ring record was (ii) then compared with the existing historic chronology to evaluate its accuracy. We finally (iii) examine the coincidence between high-magnitude avalanche occurrences and historic climate data including temperature, precipitation and snowfall, as they could enhance existing threshold values for the triggering of major avalanche events in the French Alps. Avalanche professionals and land managers can use this information in strategies for protection, forecasting as well as land-use planning and management.

2. Study site

The study was conducted at the Pierres Jean Jeanne avalanche talus slope (45°02′N/6°05′E; Fig. 1), one of the numerous avalanche paths threatening the national road in the Romanche valley. It is located on a north facing slope west of the village of La Grave, where large scree slopes are extensively forested (Corona, 2007). At Pierres Jean Jeanne, talus deposits have a width of 800 m, and are conical in form. The site has a surface area of 49 ha and is dominated by a 500-m high gneissic rockwall. From the bottom of the rockwall to the base of the slope, the difference in elevation is about 400 m (1300–1700 m asl).

The CLPA describes a triple-lobed (called L1, L2, and L3) active snow avalanche zone which coincides approximately with the vegetation-free zone below 1600 m asl (Fig. 1). A longitudinal slope profile in 10-m segments with a precision of 0.5 m was measured along the axis of L2 (Fig. 2; Corona, 2007) and analyzed with a cubic spline and its second derivative allowing for a definition of break

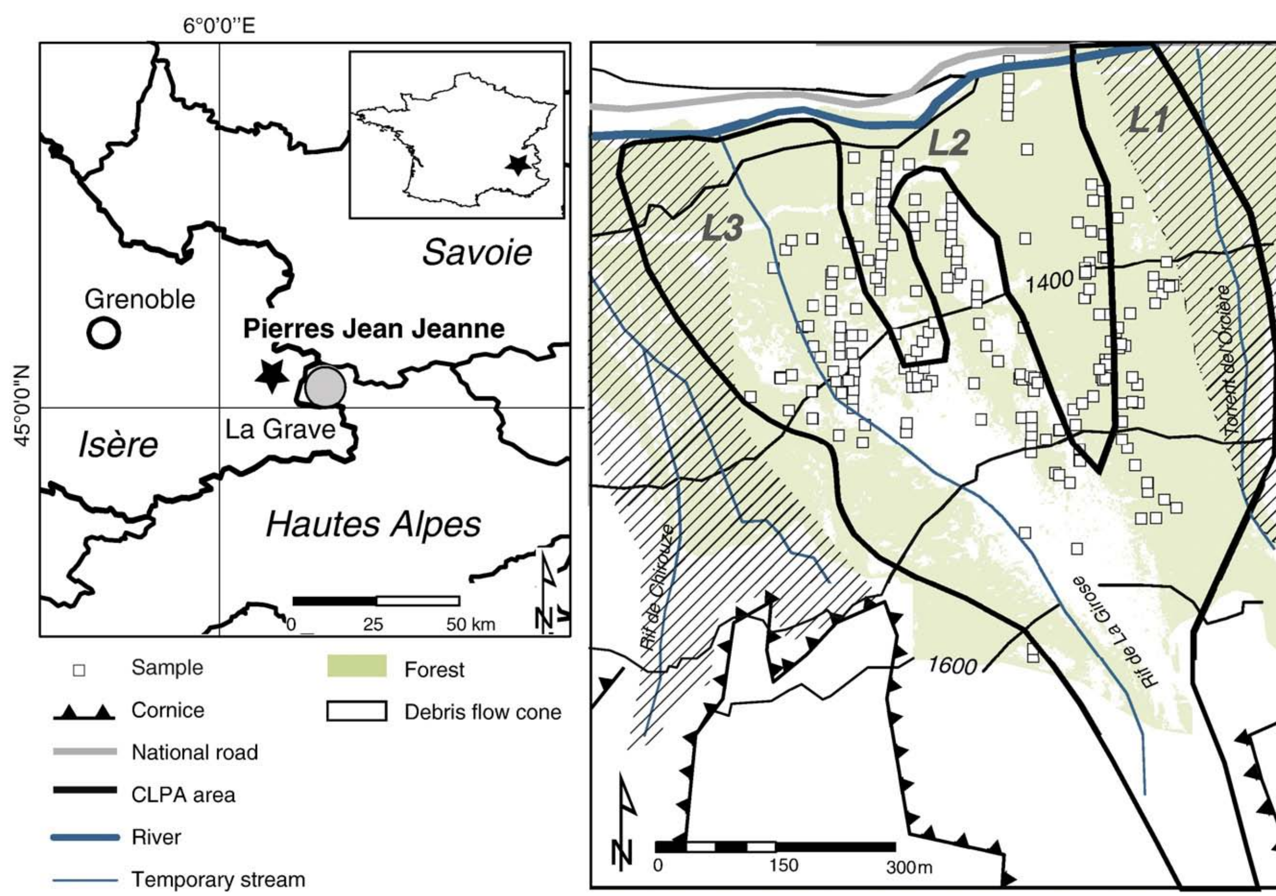

Fig. 1. The Romanche Valley and the Pierres Jean Jeanne avalanche talus slope. Map coordinates are given in latitude and longitude (WGS84).

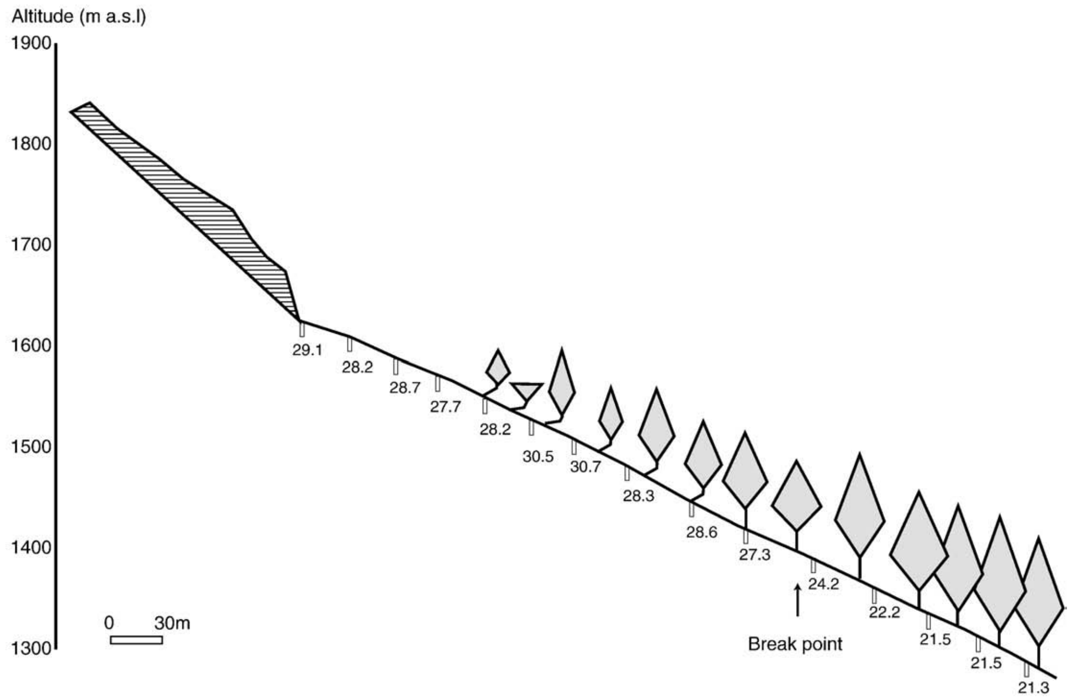

Fig. 2. Longitudinal slope profile of the Pierres Jean Jeanne avalanche talus along the axis L2 (see Fig. 1 for details). The segment inclination is given in °. Each value represents the mean of 3 consecutive measurements.

points segmenting the profile (see Francou and Manté, 1990). The mean slope angle is ~26° with a break point located at 80% of the fractionated distance from the apex at an angle of 21°. The mean slope in the upper part of the talus is lower than 34° while the distal segment appears geometrically concave with a mean slope angle slightly smaller than 20°. These values are characteristic of transition deposits for which the transit of clasts is mainly due to powerful avalanches and very rarely the result of high momentum rockfalls (Jomelli and Francou, 2000).

Located in the upper mountain stage (Ozenda, 1985), the talus deposits are covered by an open forest built of European larch (*Larix decidua* Mill.). The rate of afforestation is ~75% below 1600 m asl and increased rapidly since the early 20th century in the eastern part of the deposit at lobe L1 (Corona, 2007). In its western part (L3, Fig. 1), afforestation is much less efficient due to the repeated passage of wet-snow avalanches and deposition of avalanche deposits in the Rif de la Girose gully.

According to the data from the nearby meteorological station of Saint-Christophe en Oisans (44°57′N/6°10′E, 1570 m asl), mean annual and winter (DJF) temperatures are 6 °C and −1.4 °C, respectively, for the period 1961–2005. Mean annual precipitation is 990 mm year^{-1} (STDEV: 177 mm). Between December and April, precipitation falls primarily as snow. The records show typically 123 days with snow cover of 10 cm or more, including 92 days with more than 30 cm. Average monthly snow falls reach 46 cm with a maximum of 70 cm in February.

Archival data on past events at Pierres Jean Jeanne only covers the last 50 years. The EPA inventoried 16 events: 14 events between 1951 and 1978 (1951, 1957, 1959, 1960, 1961, 1962, 1963, 1965, 1967, 1968, 1969, 1971, 1972, and 1978), no data between 1978 and 1998, and only two avalanches since 1988, with the latest event on record in 1994. According to the EPA, the largest events would have occurred in 1961 and 1988. On 4 February 1961, a mixed (powder-flowing) avalanche destroyed 1 ha of forest and disrupted traffic on the national road. On 30 January 1988, a wet-snow avalanche destroyed electricity pylons located at 1280 m asl that were supposed to be protected by deflection dams.

3. Methods

3.1. Sampling strategy

Depending on the energy of the mechanical impact of snow and debris (i.e. rocks and boulder or broken trees) incorporated in wet avalanches, trees can be tilted, injured or broken (Bartelt and Stöckli, 2001; Mundo et al., 2007). These morphologies are associated with anatomical features, which can be detected and accurately dated in the tree-ring series using dendrochronological methods (Potter, 1969; Butler and Malanson, 1985).

A tilted tree will try to regain its vertical position producing – in the case of a conifer tree – compression wood on the tilted side of the trunk. Individual compression wood rings are considerably larger and slightly darker (i.e. yellow or brown-red) in appearance as compared to the upslope side due to the thicker and rounded cell walls of early- and latewood tracheids (Timell, 1986). When the impacting energy is important enough to locally damage cambium, increment growth will be disrupted in the injured area of the tree. In order to minimize the risk of rot and insect attacks after wood-penetrating impacts, the injured tree will compartmentalize the wound and immediately start with the production of callus tissue overgrowing scars to seal the injured tissue (Shigo, 1984; Stoffel and Bollschweiler, 2008). Moreover, certain conifer species, among which *L. decidua,* may form tangential rows of traumatic resin ducts (referred hereafter as TRD) around wounds (Bollschweiler et al., 2008b; Stoffel and Hitz, 2008; Schneuwly et al., 2009). When the windblast of a snow avalanche leads to the decapitation of the crown or to the loss of main branches, an abrupt growth reduction will appear in the tree-ring series (Butler and Malanson, 1985; Mattheck, 1996). For this investigation, we used the appearance of callus tissue and TRD, the initiation of compression wood and abrupt growth reductions to determine the occurrence of avalanches.

In the field, we sampled trees along longitudinal transects at each of the lobes L1, L2 and L3. For each transect, the trees were sampled inside and outside the delimited CLPA area. In total, we sampled 232 trees: 29 on L1, 67 on L2, 87 on L3 and 51 outside the area surveyed by the CLPA. We collected a total of 150 cross-sections from avalanche-damaged trees with poor survival probability (n = 70, 30%) and from dead *in situ* stumps (n = 80, 34%). We assumed that most dead trees were killed during past snow avalanche activity given the downslope orientation of stems. The largest trees showing obvious avalanche damage (n = 82, 35%) were sampled with a Pressler increment borer. Four cores were taken from each tree, two perpendicular to the slope and two in the flow direction of snow avalanches (i.e. in the upslope and downslope directions). This procedure helped in the detection of growth anomalies and compression wood in core samples (Reardon et al., 2008). GPS coordinates with <1 m accuracy were recorded for each tree sample using a Trimble GeoExplorer.

For each tree, additional data were collected including its position within the deposit, its diameter at breast height (DBH), description of the disturbance (i.e. amount of impact scarring, branch flagging, and tilting) and information on neighboring trees.

Sampling height was chosen according to the morphology of the stem: (i) injured or tilted trees were sampled at the height of the disturbance; (ii) cross-sections and cores from decapitated trees were, in contrast, extracted next to the stem base so as to preserve as much tree-ring information as possible (Bollschweiler et al., 2008a). In addition to the disturbed trees sampled on the cone, (iii) twenty undisturbed *L. decidua* trees showing no signs of avalanche activity or any other geomorphic process were selected outside the CLPA area. Three cores were extracted per tree, two perpendicular to the slope and one in the downslope direction.

3.2. Sample preparation and analysis

The samples obtained in the field were prepared following standard dendrochronological procedures (Bräker, 2002; Stoffel and Bollschweiler, 2009). Single steps of surface analysis included air drying of the samples, surface preparation by finely sanding, skeleton plots and ring width measurement to the nearest 0.01 mm using a digital LINTAB positioning table connected to a Leica stereomicroscope and to TSAP 3.0 software (Time Series Analysis and Presentation TSAP by Rinn, 2003).

A master tree-ring chronology was first developed based on the growth curves of the undisturbed trees using ARSTAN (Cook, 1985). A double detrending procedure (Holmes, 1994) was used with the purpose to enhance the climate signal in ring width series. First, a negative exponential curve or a linear regression line was fitted to the ring series. The second step used a cubic smoothing spline with a frequency-response cut-off set at two-thirds of the length of each series. In this way, most of the low-frequency variability in each ring series assumed to be unrelated to climate such as e.g., tree aging and forest stand development was removed (Cook and Kairiukstis, 1990).

Increment curves of the disturbed samples were then cross-dated with this reference chronology. The quality of the cross-dating was evaluated using COFECHA (Holmes, 1983). This program identifies segments within each ring width series that may have erroneous cross-dating or measurement errors on the basis of the correlations with the reference chronology and between individual series (Holmes, 1983). The purpose of this procedure was (i) to correct faulty tree-ring series derived from disturbed samples (e.g. false or missing rings; Schweingruber, 1996); (ii) to separate climatically driven fluctuations in tree growth from growth disturbances caused by avalanches (Cook and Kairiukstis, 1990), and (iii) to highlight local insect outbreaks affecting tree growth, especially larch budmoth years (*Zeiraphera diniana* Gr.).

For samples heavily impacted by multiple avalanches, avalanche "marker years" recorded in neighboring samples were used to ensure accurate calendar dating (Reardon et al., 2008). Thereafter, the samples were analyzed visually and tree rings showing TRD, the onset of compression wood or callus tissue were noted before the growth curves of the disturbed trees were compared to the reference chronology in order to determine the year of initiation of abrupt growth suppression.

3.3. Tree-ring reconstruction of avalanches

In a subsequent step, we arbitrary rated each avalanche-induced growth disturbance in each sample from 1 to 5 based on its visual quality (Germain et al., 2005; Reardon et al., 2008):

- Intensity 5: Abrupt change in radial growth associated with stem breakage, clear impact scar associated with obvious compression wood, the presence of TRD or growth suppression.
- Intensity 4: Clear scar, but no compression wood or suppression of growth or obvious compression wood that lasts for approximately three years.
- Intensity 3: Obvious compression wood during 1 or 2 successive growth years following the disturbance.
- Intensity 2: Compression wood or growth suppression present but not well defined, or, compression wood present but formed when tree was young and more susceptible to damage from various environmental and biological conditions.
- Intensity 1: Same as intensity 2 except that compression wood is very poorly defined, and slow onset may indicate other processes such as soil or snow creep as the primary causes of disturbance.

Data from individual trees was then summarized in event-response histograms (Shroder, 1978; Dubé et al., 2004; Reardon et al., 2008). For each year t, an index I was calculated based on the percentage of trees showing responses in their tree-ring record in relation to the number of trees sampled being alive in year t:

$$I_t = \left(\left(\sum_{i=1}^{n} Rt\right) \div \left(\sum_{i=t}^{n} At\right)\right) \times 100 \tag{1}$$

where R represents the response of a tree to an event in year t and A the number of trees alive in year t. Following Dubé et al. (2004) or Reardon et al. (2008), and as a result of the large sample size (Butler and Sawyer, 2008) available in the present study, the chronology of high-magnitude avalanches was based on an Index number I of 10% of all samples alive at year t. This threshold minimizes the risk that growth anomalies caused by other (geomorphic) processes could mistakenly be attributed to avalanches. We also required that a minimum of 10 trees exhibits a response so as to avoid an overestimation in the calculation of response percentage resulting from a low number of trees early in the record (Dubé et al., 2004). A major avalanche was though considered as an event with I>10% and which causes disturbances to at least 10 trees.

We are well aware that some avalanche years may be misclassified due to the strictness of the above thresholds. This is why the yearly patterns of disturbed trees were studied and why we included the position of each single tree, its years of growth disturbance as well as individual return period in our analysis. Using geographical coordinates, trees were placed into a Geographical Information System (GIS; ArcGIS 9.3; ESRI, 2005) as geo-objects and information from the database were linked as attributes to the single trees. We determined autocorrelations (feature similarity) based on the location and values of trees with the ArcGIS pattern analysis module (ESRI, 2005) and calculated yearly Moran Indices (Moran, 1950) to evaluate whether the pattern of disturbed trees was clustered, dispersed or random. A Moran Index value near 1 indicates clustering while an index value near −1 indicates dispersion. The Z scores and p-values were used to indicate the significance of individual Moran Index values and to adapt the event-response thresholds for a very limited number of particular avalanche years.

The age structure of the stand was approximated by counting the number of tree rings of selected trees and visualized after interpolation. However, since trees were not sampled at their stem base and the piths as well as the innermost rings of some trees were rotten, the age structure is biased and does not reflect inception or germination dates. Nonetheless, it may furnish valuable data on major disturbance events at the study site with reasonable precision, as *L. decidua* has been shown repeatedly to recolonize surfaces cleared by snow avalanches in the years following an event (Stoffel et al., 2006).

3.4. Calculations of avalanche return periods and extent

The avalanche frequency designates the mean time interval at which a material reaches a given point in an avalanche path (McClung and Schaerer, 1993). Frequency is usually expressed in years as a "return period" (i.e. 1/frequency). Individual tree return periods *(Rp)* were calculated from the GD frequency *f* for each tree *T* as follows (Reardon et al., 2008):

$$f_T = \left(\sum_{i=T}^{n} GD\right) \div \left(\sum_{i=T}^{n} A\right) \tag{2}$$

where GD represents the number of growth disturbances, and *A* the total number of years tree *T* was alive.

The return periods were visualized with the ArcGIS Geostatistical Analyst (ESRI, 2005) to estimate realistic values for the return period of events in areas where it could not be determined with dendrogeomorphic methods (Fortin and Dale, 2005). We then used interpolations to visualize the spatial distribution of return intervals. Following the procedure described in Johnston et al. (2003), lopsided data were first transformed to make them normal and to enhance results given by the interpolation. Trends exhibited by the data were then fitted using second-order polynomials in a southeast to northwest direction. The spherical semivariogram surface and the covariance clouds, which relate dissimilarity of data points to the distance that separates them, indicate a spatial autocorrelation in the data. As a result, the number (12) and the size (30 m) of lags have been adapted. Due to the strong directional influence (i.e. points are strongly related to those upslope of their location), anisotropy was set using an angle of 135° (approximately SE–NW) with an angle tolerance of 45° and a band width of 3. After this exploratory phase, the data were interpolated by means of an ordinary kriging model. Interpolations were performed using an ellipse-shaped search including data from five to fifteen neighboring weighted points within each of its eight sectors. In angular sections, at least two trees were taken into consideration (Stoffel et al., 2005). Finally, cross-validation was used to assess the reliability of the interpolation by comparing the measured and predicted values after sequential omission of a point. The error statistics generated for the spatial map of avalanche return periods indicates a high level of model skill and acceptable model error (Table 1).

3.5. Relationship between avalanche occurrences and climatic data

Climatic data from Météo France are used to assess relationships between avalanche occurrences and historic weather conditions. Of the stations reviewed, Saint-Christophe en Oisans (1570 m asl) provided the longest, most contiguous and reliable data source for the area, with uninterrupted values for precipitation, temperature and snowfall since 1961. Variables selected for analyses included mean monthly precipitation, snowfall, and temperature for November through May, from 1961 to 2003. Mean monthly values are considered to provide an appropriate level of resolution for analyses as dendroecological methods usually only date the year in which an avalanche event occurred (Hebertson and Jenkins, 2003).

Several Classification And Regression Tree (CART; Breiman et al., 1984; Ripley, 1996) analyses were investigated to predict major avalanche years from a set of historic climate data (Hebertson and Jenkins, 2003) using the 'rpart' routine (Therneau and Atkinson, 1997) of the R package (R Development Core Team, 2007). CART is a statistical tree-building technique that explains the variation of a response variable (i.e. avalanche indices in the present case) using a set of explanatory independent variables, so-called predictors (i.e. monthly climatic data). The method is based on a recursive binary splitting of the data into mutually exclusive subgroups within which objects have similar values for the response variable (see Breiman et al., 1984 for details). At each split, CART imposed a "goodness of split criterion", similar to the method of least squares, so as to optimize splitting for each variable and ultimately minimizing the overall probability of misclassifying the response variable. CART added variables until classification trees were grown to a maximum size and in the final step removed those variables that contributed no predictive power to the model. This allowed CART to select the best models adjusting for the number of variables used in the analysis (Hebertson and Jenkins, 2003).

Several CART models were tested with different combinations of predictors and years from 1961 to 2003 and grouped into two response classes. Years with avalanche indices $<10\%$ were class 0, and years with avalanche indexes $>10\%$ were class 1.

The relation between climatic variables and avalanche initiation was further explored by using logistic regressions (Aldrich and Nelson, 1984; Hebertson and Jenkins, 2003). This method describes the relationship between a dichotomous response variable, the presence or absence of an avalanche event in our case, and a set of explanatory variables, the climatic data herein. Logistic regression addresses the same questions as least squares regression (OLS) but provides a more robust method for modeling probabilities when the dependent variable takes on only two values (0, 1). This is primarily because the OLS linear probability model is heteroscadastic and may predict probability values beyond the (0, 1) range (Hebertson and Jenkins, 2003). In this analysis, the probability of major avalanche years was the dependent variable with major avalanche years identified by means of tree-ring analysis equal to 1, and otherwise 0. In logistic regression, however, one estimates the probability that the outcome variable assumes a certain value, rather than estimating the value itself by fitting data to a logistic curve. The logit is simply the log odds ratio of mean avalanche probability:

$$\text{logit}(p_i) = \left(\frac{p_i}{1-p_i}\right) \tag{3}$$

where p is the probability of a major avalanche year for the i years (1961–2003 herein).

It is modelled as a linear function:

$$\text{logit}(p_i) = \beta_0 + \beta_1 x_{1,i} + \ldots + \beta_k x_k, i \tag{4}$$

with an equivalent formulation:

$$p_i = \frac{1}{1 + e^{-(\beta_0 + \beta_1 X_{1,i} + \ldots + \beta_k X_k, i)}} \tag{5}$$

where X_k represents the k climatic factors used as regressors for year i, β_0 the intercept and β_k the regression coefficients.

Table 1
Cross-validation statistics and model error coefficients for the kriged return period map (Fig. 7). Models providing accurate predictive capabilities should exhibit mean error values close to 0, root-mean squared error and standard error should be as small as possible, and the root-mean-square standardized error should be close to 1.

Error metric	Value
Mean	0.3549
Root-mean-square	2.06
Average standard error	0.81
Mean standardized	0.02592
Root-mean-square standardized	3.451

The unknown parameters βj are usually estimated by a maximum likelihood using a method common to all generalized linear models. Using the SYSTAT procedure, an initial logistic regression model was fit with all climate variables and subsequently backward elimination was used to derive the most parsimonious model.

4. Results

4.1. Age structure of the stand

Visual cross-dating was carried out by means of the skeleton plot method and primarily based on the narrow rings of 1906, 1937, 1946, 1956, 1962, 1972, 1983 and 1986 (Fig. 3). After cross-dating, data on the pith age at breast height indicates that the 232 European larch (*L. decidua* Mill.) trees growing on the Pierres Jean Jeanne avalanche talus are on average 63 years old (STDEV: 20 years). The oldest tree selected for analysis attained sampling height in AD 1857 while the youngest only reaches breast height in 1991. As can be seen from Fig. 4, the sectors located in the axis of L2 and L3 frequently contain trees aged between 25 and 40 years.

According to tree-ring data, seedlings started to recolonize the talus cone in these two areas between the 1960s and 1980s. This spatially homogeneous distribution of tree ages suggests that parts of the stand must have been eliminated through large snow avalanches in the past. Below 1400 m asl, in the portions of the talus located between L1 and L2, between L2 and L3, and in the central part of L3, trees reach an average of 80 years and seem to be reasonably well protected from recent snow avalanche activity.

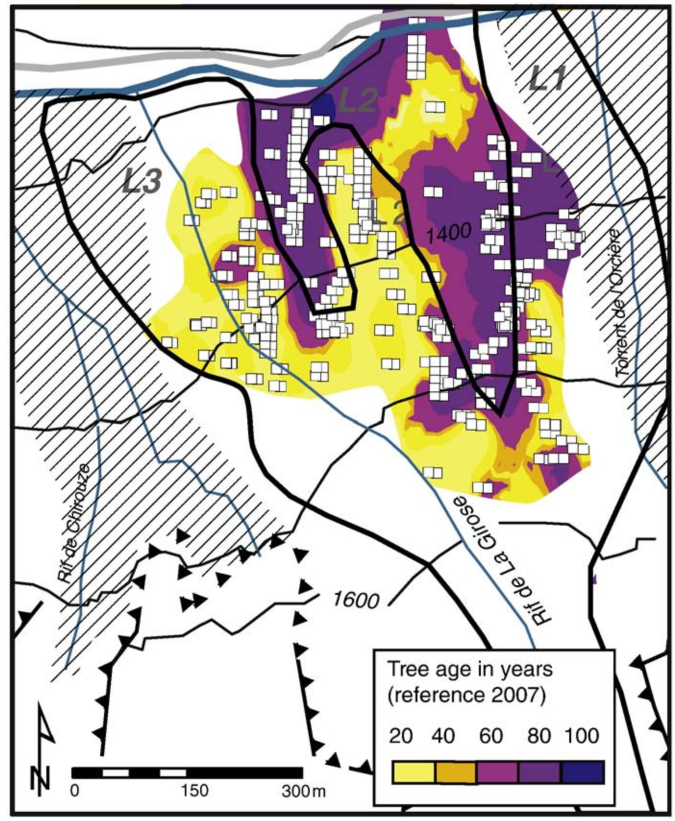

Fig. 4. Age structure of the forest stand growing on the Pierres Jean Jeanne avalanche talus.

4.2. Growth disturbances in trees

The 374 samples (224 increment cores and 150 cross-sections) selected from the 232 *L. decidua* trees permitted identification of 901 growth disturbances (GD). Their intensity reactions are summarized in Table 2. Tangential rows of traumatic resin ducts (TRD) following cambium wounding and the onset of compression wood after tilting were commonly found in the samples, but callus tissue, abrupt growth releases or growth reductions could be identified as well (Table 2).

In 1912, the sample size surpassed the n = 10 trees threshold for GD to be considered an avalanche event using dendrogeomorphic methods (Fig. 5a and b). Sample size increased markedly after 1935 and surpassed 50% (n = 116) in 1943. The earliest GD in the tree-ring series occurred in 1903 and 1904. GD became more frequent after 1919, and nearly every year exhibited GD in a small number of trees. Most of these years were not classified as avalanche years because fewer than 10 trees and less than 10% of the samples alive that year showed reactions. Snow creep or rockfalls may account for many of these responses. In total, GD did exceed the 10%-thresholds in 18 years after 1919 and all of these years were considered avalanche years: 1919, 1921, 1927, 1929, 1932, 1935, 1937, 1940, 1941, 1947, 1961, 1969, 1971, 1978, 1981, 1985, 1988, and 1994. In addition, 1951 and 1959 were accepted as additional avalanche years because they were very close to the threshold and because historic records indicate avalanche activity during these winters.

The years 1981 (n = 125), 1971 (n = 87), 1994 (n = 52), 1961 (n = 50) are those exhibiting the greatest number of trees showing GD (Fig. 5a). In a similar way, the highest frequency of appearance is measured in 1981 (58%), 1971 (41%), 1927 (35%) and 1961 (27%). The distribution of avalanche years proves to be relatively homogeneous with 2 to 3 avalanche episodes per decade. At the same time, however, we observe lags in avalanche activity recorded in the trees between 1951 and 1961 and since 1994.

4.3. Spatial distribution of trees affected by avalanche events

The spatial distribution of trees affected by the same event is of considerable help for the determination of the minimum spatial extent of past avalanches. The reconstructed maps, provided in Fig. 6, clearly indicate that the lateral extent of the events varies according to five general patterns: (i) In 1919, 1921 and 1937, avalanches are restricted to L1; (ii) the events in 1929, 1932, 1940 and 1985, in contrast, affected trees located in the central part of the cone, approximately along the axis of L2. We also observe (iii) three avalanches (1927, 1941, and 1947) that are limited to the eastern part of the cone (L1 and L2) prior to AD 1950, whereas (iv) events restricted to the western segments of the talus cone

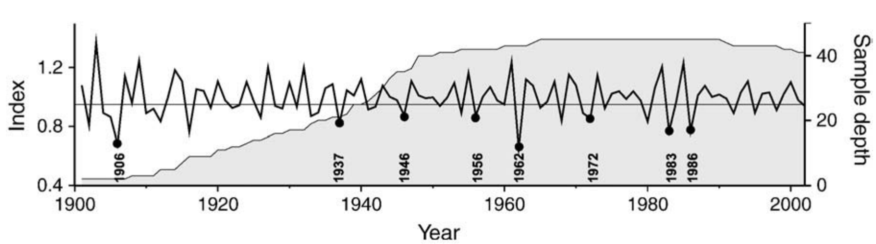

Fig. 3. Tree-ring chronology of European larch (*Larix decidua* Mill.) for the upper Romanche valley dating back to AD 1900. Individual series are detrended with (i) a negative exponential curve or a linear regression and (ii) by a cubic smoothing spline function. The sample depth is indicated in grey.

Table 2
Intensity reactions and types of growth disturbances (GD) assessed in the 232 *Larix decidua* Mill. trees selected for analysis.

Intensity	Number	%	Type	Number	%
1	25	3	Tangential rows of traumatic resin ducts	361	40
2	101	11	Compression wood	342	38
3	267	30	Callus tissue	108	12
4	354	39	Growth reduction	90	10
5	154	17			
Total	901	100		901	100

only occurred after 1969 (1969, 1978). Finally, (v) four events affected trees throughout the cone in 1961, 1971, 1988 and 1994.

The yearly Morans I statistics vary between −0.22 in 1914 (i.e. dispersed distribution of affected trees) and 0.58 in 1962 (i.e. spatial clustering of GD). Among the 20 reconstructed events, 16 display significant clustered patterns of affected trees with a maximal aggregation in 1919, 1932 and 1927. In contrast, four avalanche years (20%) display no significant pattern. Only 10 non-avalanche years (17%) portray a pattern with clustered disturbed trees. Interestingly, four of them (1933, 1960, 1962, and 1995) are observed in the year following major avalanche activity. In these cases, the clustering is probably related to remaining disturbance signaling (i.e. persistence of TRD formation, delayed compression wood formation, delayed growth change, etc.).

4.4. Estimates of avalanche return periods and return period mapping

The average return period of snow avalanches for the entire study site was calculated for five time intervals (Table 3): (i) the entire length of the chronology (i.e. historic and tree-ring records, 1912–2007), (ii) the period for which sample depth was >10 trees but historic records were scarce (1912–1951), (iii) the period for which sample depth was >10 trees but the EPA was fairly documented (1952–2007), (iv) the period for which snowpack records are available (1964–2007), and (v) the period containing recent climate warming in the Alps (1981–2007). For these five intervals, calculated return periods of snow avalanches range from 3.6 to 6.8 years with an overall average of 4.8 years.

Within the area sampled, the return periods increased rapidly with distance downslope, particularly in the eastern part of the deposit (Fig. 7). The map of avalanche frequencies at the study site showed calculated return periods (1/f) ranging from 15 years in the lower part of L3 (i.e. in the axis of the Rif de la Girose) to 50 years in the lower part of L2. The horizontal distance between these points is ~300 m, with only a slight change in elevation. Longitudinally, the return period increases gradually in the axis of L2 from 2.5 years in the upper part of the lobe to 25–50 years in its lower part. Elsewhere, the increase in return periods occurs in two steps: the return period almost doubles between 1500 (10.5 years) and 1450 m asl (17 years) and increases rapidly to 50 years at ~1350 m asl.

4.5. Snow avalanches/climate relationships

The best model deriving from the CART analysis used only mean monthly December and January snowfalls to optimize the splitting of major avalanche year probabilities. The splitting value for mean monthly December–January snowfall was 167.5 cm. For this model, CART also selected closely associated mean monthly December–January temperatures with splitting values of −1.4 °C that could be used for further analyses or discussion. Cross-validation classification

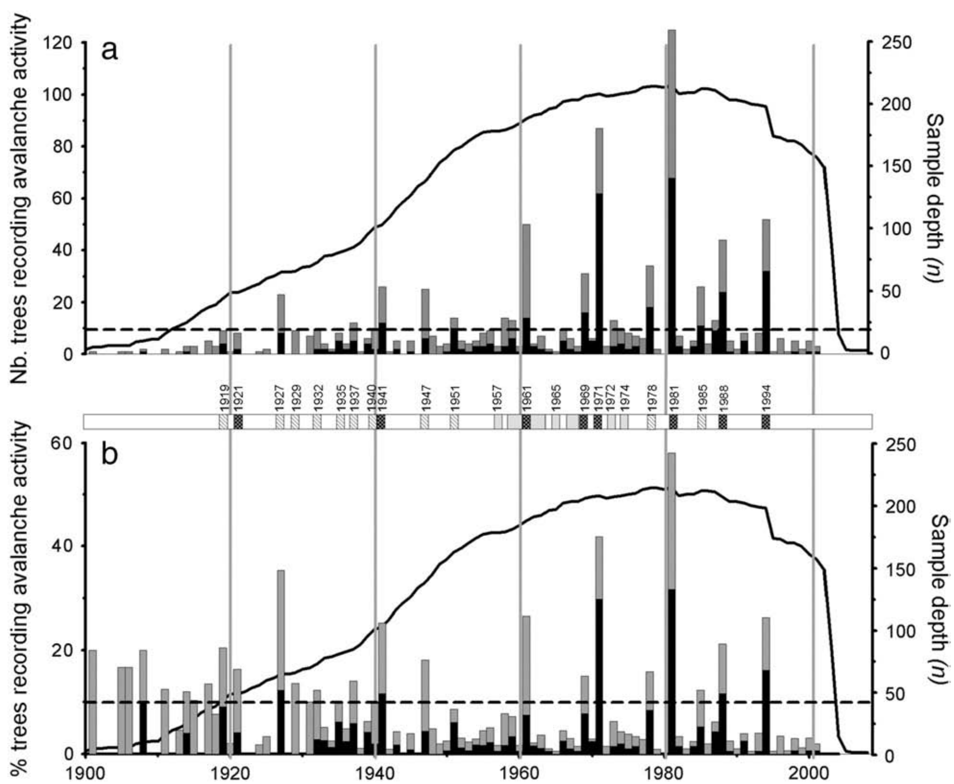

Fig. 5. Event-response histograms showing avalanche-induced growth responses from sampled trees, and historic avalanche events. (a) Total number of trees, and (c) the percentage of trees responding to a damage event. Stacked bar graphs show the proportion of samples classified as high- (4–5, dark shading) and low-quality (1–3, light shading) using the tree growth response rating system. Horizontal dotted line demarcates, in (a), the n = 10 tree threshold, and, in (b), the 10% of sample depth thresholds. The grey line shows the total number of trees (n) alive each year. Avalanche events reconstructed from both the historic record and dendrogeomorphic analysis are identified using a black diagonally cross-hatched box. Possible avalanche events reconstructed with dendrogeomorphic methods are identified using a white-hatched box, avalanche events listed in the EPA with a dotted box.

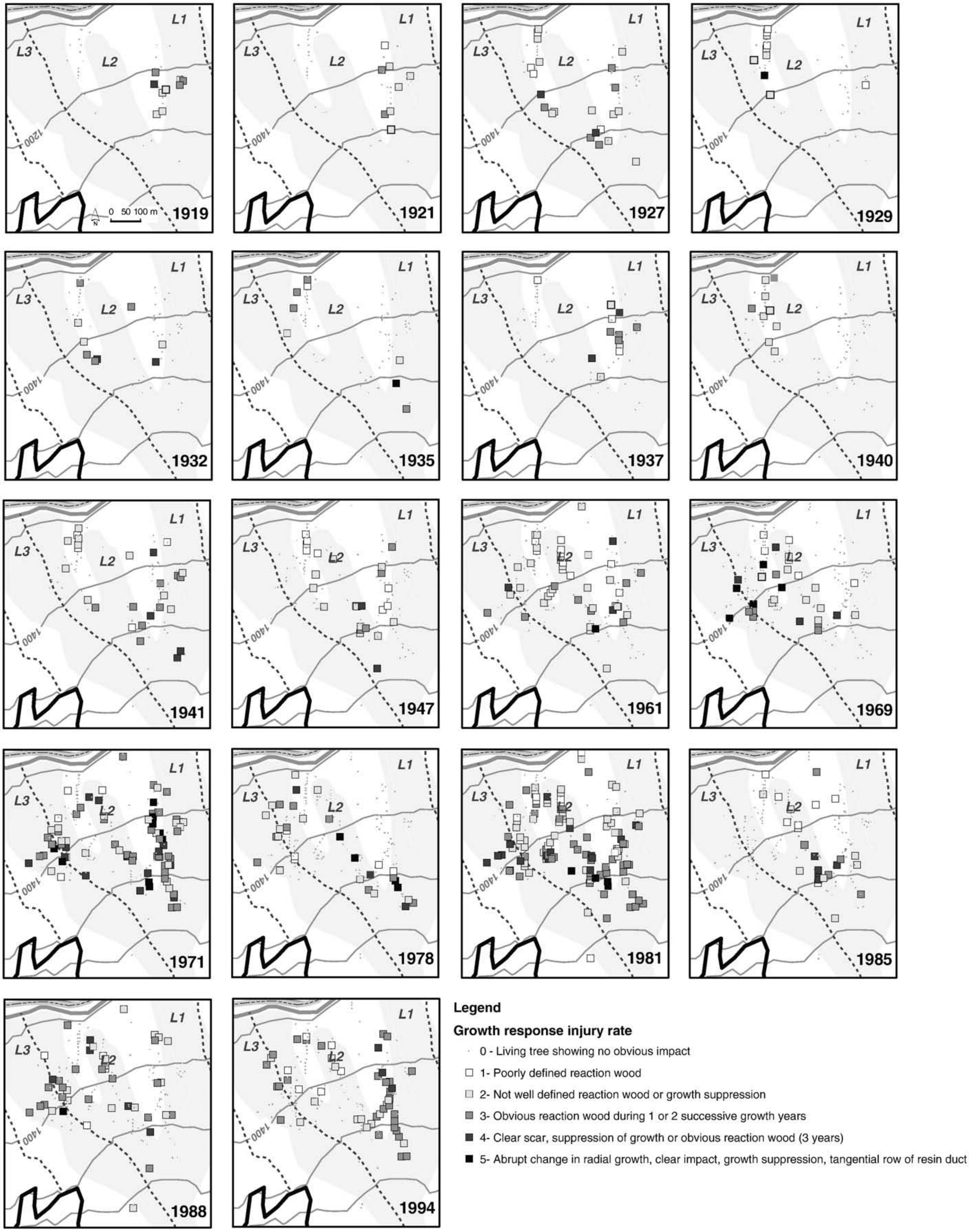

Fig. 6. Reconstructed minimum slide extents for the 18 avalanche years. Maps show living trees and all trees showing an event-response for the year of the avalanche. The grey shading denotes the CLPA area.

Table 3
Return periods of reconstructed snow avalanches at Pierres Jean Jeanne for five time intervals. The five intervals cover (i) the entire length of the record, (ii) the years early in the chronology when the historic record is limited, (iii) the years for which sample depth is >10 trees and the EPA is fairly well documented, (iv) the years for which snowpack records are available from Saint-Christophe en Oisans and (v) the period of recent climate warming in the Alps.

Interval	Years	Avalanches	Return period
1912–2007	96	20	4.8
1912–1951	40	11	3.6
1952–2007	56	9	6.2
1964–2007	44	7	6.4
1981–2007	27	4	6.8

probabilities indicated that the model correctly classified non-avalanche years 90% of the time. The likelihood of correctly classifying major avalanches years, however, is only 60%. The most parsimonious logistic regression model after backward elimination has the general form:

$$\mathrm{Logit}(p_i) = \beta_0 + \beta_j(\textit{December} + \textit{January snowfall})$$

The model provides parameter estimates of -4.75 for β_0 and 0.033 for β_j. In other words, β_j indicates that the probability of a major avalanche year was estimated to increase by 0.033 with a respective 1 cm increase in mean December + January snowfall. The chi-square statistics for β_0 and β_j are 14.52 and 10.53, respectively, both highly significant with $p<0.0001$. The likelihood ratio test, significant at $p<0.0001$, indicates that the logit is better than a null model and the Pseudo-R^2 value (0.32) in correctly predicting avalanche triggering probability. The model properly classifies 62% of the avalanche years and 95% of the non-avalanche years. The probability of a major avalanche is 4% for 50 cm December + January snowfall, 19% for 100 cm snowfall and 54% for 150 cm snowfall. It reaches 86% when snowfall totals exceed 200 cm (Fig. 8).

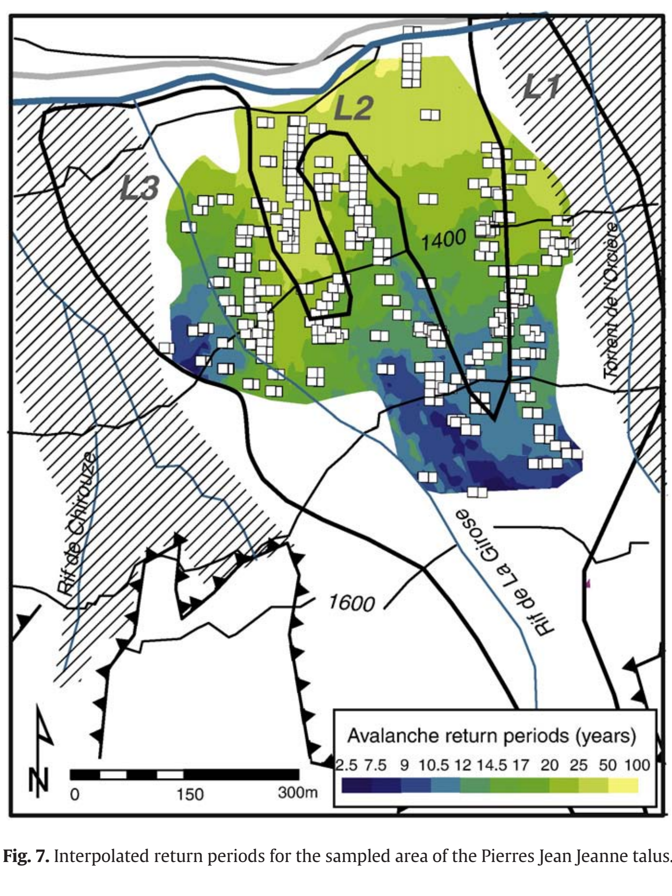

Fig. 7. Interpolated return periods for the sampled area of the Pierres Jean Jeanne talus.

5. Discussion

5.1. Temporal accuracy of the reconstruction

In this study, a dendrogeomorphic approach was used to reconstruct 20 avalanche events. The reconstruction complemented the existing avalanche chronology back to 1912, added nine events which were previously unknown for the time before 1951 and two events for the period with archival records (1951–2003). The national avalanche authority EPA confirms seven of the reconstructed avalanche years between 1951 and 1994: 1959, 1961, 1969, 1971, 1978, 1988, and 1994. Five other events are indirectly confirmed via historical data on intense avalanche activity in the Oisans Massif region, namely the avalanches of 1919, 1921, 1927 (Allix, 1929), 1941 (MEDD, CEMAGREF, ONF, 2006), and 1981 (Ancey, 1998; Villecrose, 2001).

Although eight events remain unconfirmed, the reliability of our reconstruction is enhanced by the methodology deployed in this study. The two thresholds (i.e. GD in 10% of the samples present at the time of the event and a minimum number of 10 trees showing GD) minimized the likelihood that GD resulting from non-avalanche events were included in the chronology (Reardon et al., 2008). The thresholds also allowed rejection of GD related to other geomorphic processes such as snow creep or rockfall which have been shown to affect a rather limited number of trees per event (Stoffel and Perret, 2006). For years with exceedances of the thresholds, the presence of clearly visible physical evidence of impacts in the form of injuries and/or severe growth responses (i.e. intensity 4 and 5 reactions) as well as the spatial autocorrelation analysis of GD was used as further criteria for an undoubtful dating of snow avalanche events.

However, the comparison between historic and tree-ring records at Pierres Jean Jeanne suggests that the dendrogeomorphic reconstruction underestimates years with natural avalanche activity by roughly 50%. For several reasons, the number of reconstructed snow avalanches has to be seen as a minimum frequency of natural avalanches. First, avalanches have to be of sufficient magnitude to have ecological impacts on the vegetation and it can be expected that only the events of destructive class 2 or larger (McClung and Schaerer, 1993; Reardon et al., 2008) with a typical mass $>100\ \mathrm{m}^3$, a path length >100 m and an impact pressure >100 kPa will emerge from the tree-ring record.

In addition, it seems obvious that the limited number of trees available prior to 1935 will influence the quality of the reconstructed frequency. While the methodology applied in this study minimizes the risk of including non-avalanche events in the chronology, it most likely also creates a bias towards larger avalanches, as smaller snow avalanches or events limited to the non-forested parts of the

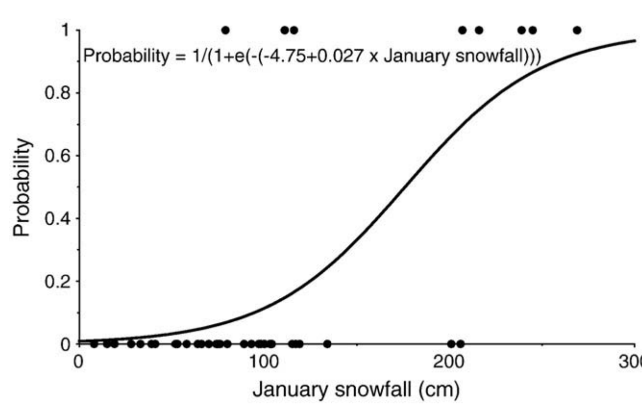

Fig. 8. Mean December + January snowfall values and predicted probabilities of major avalanche years for the Pierres Jean Jeanne talus.

avalanche talus cone cannot be identified by means of tree-ring analysis. This fact is supported by archival data for the events of 1951, 1957, 1960, 1965 and 1975, where the EPA notes the presence of snow avalanches with limited extension. These events do not therefore appear in the tree-ring based reconstruction, since the number of GD observed in the tree-ring series did not exceed the threshold.

Finally, major avalanches may remove or blur the evidence of previous or subsequent events in case large parts of the forest are destroyed (Carrara, 1979; Bryant et al., 1989) or disturb tree growth in such a way that younger events cannot be identified in the tree-ring record. For example, we find a large number of trees showing GD as a result of the avalanche activity of 1961 and 1971, but fail to identify the events of 1962 and 1972, known from the EPA database. These results emphasize the necessity to combine historic with dendrogeomorphic analyses when assessing avalanche hazards and risks.

5.2. Spatial accuracy of the reconstruction

The age structure of the forest stand at Pierres Jean Jeanne clearly shows that the oldest trees are located in the central segment of the eastern part as well as in the lower parts of the avalanche talus whereas trees in the upper and western parts are much younger. This pattern is consistent with the map of snow avalanche return periods. Trees growing in the uppermost part of the cone and in its western part, near Rif de la Girose, are regularly eliminated by snow avalanches with sub-decadal return periods. In contrast, trees growing in the lower part of the cone seem to be somehow more protected from avalanche influence, as events return at a multi-decadal scale.

The reconstruction spatially matches with historical archives concerning the longitudinal extents of past events. Thus, the avalanche of 1921, described in Allix (1923), extended over the Romanche River and disrupted the national road. Similarly, according to Blanchard (1943), the avalanche of 1941 has left snow deposits near the national road. For both events, our reconstruction indicates disturbances in trees located in the lowermost part of L2. Since 1959, the EPA specifies ten events that reached 1200 m asl, among those the snow avalanches of 1959, 1961, 1969, 1971, 1988, and 1994 are reported in our maps with a considerable longitudinal extents.

Yet, the lateral extent of past avalanches remains poorly documented in historic records as well as in the EPA. Large discrepancies exist between the lateral limits derived from the dendrogeomorphic approach and the data reported in the CLPA. Particularly, several events are reconstructed in the “avalanche-free” areas reported in the CLPA between L1/L2 (Fig. 5) and between L2/L3. According to Reardon et al. (2008), this lateral variability could result from meteorological factors, such as snowfall or windloading, that determine the amount of snow involved in natural avalanches, or from deflection that occurs when multiple avalanches run in a single winter and existing debris influences the direction of subsequent avalanche flow. These findings clearly demonstrate the contribution of tree-ring studies to avalanche mapping.

5.3. Climate influence on avalanche frequency

Analyses of the meteorological datasets spanning more than forty years (1961–2003) indicated that mean December and January snowfalls were significantly related to the probability of major avalanche years on the cone. The highest probabilities of major avalanche years generally corresponded with high mean December + January snowfall, while low snowfall resulted in relatively low probabilities. Archival data and the EPA help in the accurate dating of eight events, namely 26/01/1921 (Allix, 1929), 29/12/1959, 04/02/1961, 28/12/1969, 24/03/1971, 28/01/1978, 30/01/1988 and 07/01/1994. They confirm the importance of December and January snowfalls for avalanche releases in six out of eight events. We consider this a reasonable result because (i) surface roughness features cannot serve as anchors in avalanche starting zones and tracks when a thick snow cover prevails and as (ii) friction for moving snow is limited (Hebertson and Jenkins, 2003). The loading due to substantial early winter snow might also favor the initiation of sizable avalanches (McClung and Schaerer, 1993) and with the release, thick snow covers maximize the additional entrainment snow, thus increasing the size of avalanches (Hebertson and Jenkins, 2003).

An accurate examination of the snowfall dataset enables assessment of the thresholds provided by the model for triggering. It reveals high three-day intensities in December or January for seven dated events. The minimal threshold for triggering (55 cm from 27 to 29 January 1988) is within the 90% quantile (q_{90}) of the whole distribution. High three-day snowfall amounts are also recorded in 1961 (84 cm from 1 to 3 February 1961), 1969 (116 cm from 22 to 24 December 1968), 1978 (67 cm from 22 to 24 January 1978) and in 1994 (82 cm from 22 to 24 December 1993). It is also worthwhile to note that 65 cm of snow were recorded at the Bérarde weather station (located 12 km to the south of the snow avalanche talus cone) in just one day in January 1921 (Allix, 1929). These results confirm the correlation between avalanche occurrence and the total precipitation for the three days preceding a given avalanche event (Butler, 1986; De Quervain and Meister, 1987; Jomelli et al., 2007). The large amounts of fallen snow over a short period overload weak layer within the snowpack and increase its downslope deformation (McClung and Schaerer, 1993). The intensities that trigger an avalanche are in close agreement with the values recognized by meteorologists. If we take into account that the 55 cm of snow recorded in January 1988 were predated by 37 cm from 20 to 22 January, then the thresholds (100 to 120 cm) commonly recognized as a condition to trigger an exceptional avalanche (Poggi and Plas, 1969; Villecrose, 2001) are practically reached.

These snowfalls occur at the beginning of winter and are generally associated with negative temperature anomalies, as observed in January 1961 (−0.7 °C, if compared to the average 1951–2000), December 1969 (−2.1 °C), January 1978 (−0.8 °C) and December 1993 (−1 °C). Such anomalies might induce high temperature gradients and a steep snow metamorphism causing the formation of depth hoar and faceted crystal layers in thin early winter snowpacks, i.e. fragile layers that regularly account for high-magnitude avalanches and large numbers of fatalities (McClung and Schaerer, 1993).

6. Conclusion

Because of increased human activity in mountain areas, it has become imperative to improve avalanche forecasting at the local level, which is currently difficult to attain using physical models alone. We demonstrate that dendrogeomorphic methods are a powerful tool for the analysis of past snow avalanches on forested avalanche talus cones. The results presented in this study show that dendrogeomorphic analysis clearly has the potential to reconstruct past avalanche events and to add substantially to the historic record for this area.

In addition, dendrogeomorphic data can add evidence to the extent of past events where other sources often fail to produce conclusive results. The method enables an accurate mapping of both events and return periods. The comparison with the CLPA clearly demonstrates that the spread and reach can be better defined resulting in reduced evaluations. For land-use planning, the identification of the area in danger is of paramount importance. In hazard zoning, dendrogeomorphic mapping should be used systematically where woody vegetation isavailable. Finally, it can improve our knowledge of the causes of snow avalanche activity in relation to meteorological parameters, which is of interest to all those in charge of anticipating avalanche potential on multi-annual to multi-decadal timescales.

Nonetheless, refining the methods used within this study could be accomplished by (i) focusing on avalanche talus cones with accurately documented EPA covering a long period of the past, (ii) replicating studies for a larger number of avalanche talus cones, (iii) using weather station instrumentation at remote sites, calibrated against long meteorological time series, to obtain more relevant data for modeling, (iv) trying to identify anatomical differences related to dense and powder avalanches so as to allow differentiation of both processes, and (v) comparing the return period maps reconstructed by means of tree-ring analysis with estimated return periods as a function of position estimated with various models (Föhn, 1978; McClung, 2000).

Acknowledgements

The authors gratefully acknowledge Jessy Andreau for the assistance in the field. The authors also want to thank the Parc Naturel des Ecrins and the Office National des Forêts for sampling permissions. This research has been supported by the PARAMOUNT program (2-2-2-AT), " Improved Accessibility, Reliability and security of Alpine transport infrastructure related to mountainous hazards in a changing climate ", funded by the Alpine Space Programme, European Territorial Cooperation, 2007-2013. It has also been supported by the DENDRO-GLISS program, funded by the MAIF foundation and the Cemagref.

References

Aldrich, J., Nelson, F., 1984. Linear Probability, Logit and Profit Models. Sage Publications, Beverly Hills, CA.
Allix, A., 1923. Les avalanches de l'hiver 1922–23 en Dauphiné. Revue de Géographie Alpine 11, 513–527.
Allix, A., 1929. Un pays de haute montagne : l'Oisans, étude géographique. Laffite, Marseille.
Ancey, C., 1998. Guide neige et avalanches - Connaissances, pratiques, sécurité. Edisud, France.
Bartelt, P., Stöckli, V., 2001. The influence of tree and branch fracture, overturning and debris entrainment on snow avalanche flow. Annals of Glaciology 32, 209–216.
Bezzi, M., Cantiani, M.G., Ciolli, M., Comunello, G., Cherubini, P., 2003. Leggere gli anelli degli alberi per ricostruire la frequenza e l'estensione delle vlanghe nel passato. In: De Angelis, P., Macuz, A., Bucci, G., Mugnozza, G.S. (Eds.), Atti del III Congresso Nazionale: Alberi e foreste per il nuovo millennio. Viterbo, Società Italiana di Selvicoltura ed Ecologia Forestale, pp. 147–152.
Blanchard, R., 1943. Les Alpes occidentales. Les Cluses préalpines et le Sillon alpin, Tome 2. Arthaud, France.
Bollschweiler, M., Stoffel, M., Schneuwly, D.M., Bourqui, K., 2008a. Traumatic resin ducts in *Larix decidua* stems impacted by debris flows. Tree Physiology 28, 255–263.
Bollschweiler, M., Stoffel, M., Schneuwly, D.M., 2008b. Dynamics in debris-flow activity on a forested cone—a case study using different dendroecological approaches. Catena 72, 67–78.
Bräker, O.U., 2002. Measuring and data processing in tree-ring research—a methodological introduction. Dendrochronologia 20, 203–216.
Breiman, L., Friedman, J.H., Olshen, R.A., Stone, C.J., 1984. Classification and Regression Trees. Wadsworth & Brooks/Cole Advanced books & software.
Bryant, C.L., Butler, D.R., Vitek, J.D., 1989. A statistical analysis of tree-ring dating in conjunction with snow avalanches: comparison of on-path versus off-path responses. Environmental Geological Water Science 14, 53–59.
Butler, D.R., 1986. Snow-avalanche hazards in Glacier National Park, Montana, meteorologic and climatologic aspects. Physical Geography 7, 72–87.
Butler, D.R., Malanson, G.P., 1985. A history of high-magnitude snow avalanches, southern Glacier National Park, Montana, U.S.A. Mountain Research and Development 5, 175–182.
Butler, D.R., Sawyer, C.F., 2008. Dendrogeomorphology and high-magnitude snow avalanches: a review and case study. Natural Hazards and Earth System Sciences 8, 303–309.
Carrara, P.E., 1979. The determination of snow avalanche frequency through tree-ring analysis and historical records at Ophir, Colorado. Geological Society of America Bulletin 90, 773–780.
Casteller, A., Stöckli, V., Villalba, R., Mayer, A.C., 2007. An evaluation of dendroecological indicators of snow avalanches in the Swiss Alps. Arctic, Antarctic, and Alpine Research 39, 218–228.
Comunello, G., Bezzi, M., Cherubini, P., Ciolli, M., Cantiani, M.G., 2001. Conoscere il passato per interpretare il presente: tecniche GIS e di dendrocronologia applicata per lo studio di aree potenzialmente soggette al rischio di valanghe. Linea Ecologica 4, 58–62.
Cook, E.R., 1985. A time series analysis approach to tree-ring standardization. PhD Dissertation, University of Arizona, Tucson, AZ, USA.
Cook, E.R., Kairiukstis, L., 1990. Methods of Dendrochronology. Kluwer, Dordrecht.
Corona, C., 2007. Evolution biostasique du paysage, géodynamique nivéo-périglaciaire et fluctuations climatiques récentes dans la haute vallée de la Romanche (Alpes du Nord France). Ph.D. Thesis, Univ. Joseph Fourier, Grenoble.
De Quervain, M., Meister, R., 1987. 50 years of snow profiles on the Weissfluhjoch and relations to the surrounding avalanche activity (1936–1985). Proceedings of the IAHS symposium, Davos, IAHS pub, 162, pp. 161–181.
Decaulne, A., Saemundsson, T., 2006. Geomorphic evidence for contemporaneous snow-avalanche and debris-flow impact in the Icelandic Westfjords. Geomorphology 80, 80–93.
Didier, L., Brun, J.J., 1998. Limite supraforestière et changements environnementaux : pour une approche pluriscalaire et spatialisée des écosystèmes d'altitude. Géographie Physique et Quaternaire 52, 245–253.
Dubé, S., Filion, L., Hétu, B., 2004. Tree-ring reconstruction of high-magnitude snow avalanches in the northern Gaspé Peninsula, Québec, Canada. Arctic, Antarctic, and Alpine Research 36, 555–564.
Durand, Y., Giraud, G., Brun, E., Mérindo, L., Martin, E., 1999. A computer-based system simulating snowpack structures as a tool for regional avalanche forecasting. Journal of Glaciology 45, 469–484.
ESRI (Environmental Systems Research Institute), 2005. ArcGIS 9.2, Redlands, California (1992–2006).
Föhn, P.M.B., 1978. Avalanches frequency and risk estimation in forest sites. Proceedings of Seminar of the International Union of Forestry Research Organizations, Davos, Switzerland, September, pp. 241–254.
Fortin, M., Dale, M., 2005. Spatial Analysis: a Guide for Ecologists. Cambridge University Press, Cambridge.
Francou, B., Manté, C., 1990. Analysis of the segmentation in the profile of Alpine talus slopes. Permafrost and Periglacial Processes 1, 53–60.
Frazer, G.W., 1985. Dendrogeomorphic Evaluation of Snow Avalanche History at Two Sites in Banff National Park, Unpublished M.Sc. thesis, Department of Geography, University of Western Ontario, London, ON, Canada.
Germain, D., Filion, L., Hetu, B., 2005. Snow avalanche activity after fire and logging disturbances, northern Gaspé Peninsula, Quebec, Canada. Canadian Journal of Earth Sciences 42, 2103–2116.
Glass, B., Huet, P., Rat, M., Tordjeman, R., 2000. Retour d'expérience sur l'avalanche du 9 février 1999 à Montroc, commune de Chamonix après la phase contradictoire. Ministère de l'aménagement du territoire et de l'environnement. Inspection générale de l'environnement, France.
Gruber, U., Margreth, S., 2001. Winter 1999: a valuable test of the avalanche-hazard mapping procedure in Switzerland. Annals of Glaciology 32, 328–332.
Hebertson, E.G., Jenkins, M.J., 2003. Historic climate factors associated with major avalanche years on the Wasatch Plateau, Utah. Cold Regions Science and Technology 37, 315–332.
Holmes, R., 1983. Computer-assisted quality control in tree-ring dating and measurement. Tree-ring Bulletin 44, 69–75.
Holmes, R., 1994. Dendrochronology Program Library User's Manual. Laboratory of Tree-Ring Research University of Arizona, Tucson.
Jamard, A.L., Garcia, S., 2002. L'enquête permanente sur les avalanches (EPA). Statistique descriptive générale des événements et des sites. Ph.D. Thesis, Univ. Joseph Fourier, Grenoble.
Johnston, K., Ver Hoef, J.M., Krivoruchko, K., Lucas, N., 2003. Using ArcGIS Geostatistical Analyst. Environmental Systems Research Institute (ESRI), Redlands, CA, USA.
Jomelli, V., Francou, B., 2000. Comparing characteristics of rockfall talus and snow avalanche landforms in an alpine environment using a new methodological approach. Geomorphology 35, 181–192.
Jomelli, V., Delval, C., Grancher, D., Brunstein, D., Escande, S., Hétu, B., Filion, L., Pech, P., 2007. Probabilistic analysis of snow avalanches and climate relationships in the French Alps since the 1980s. Cold Region Science and Technology 47, 180–192.
Mattheck, G.C., 1996. Trees—the Mechanical Design. Springer-Verlag, Berlin.
McClung, D., 2000. Extreme avalanche runout in space and time. Canadian Geotechnical Journal 37, 161–170.
McClung, D., Schaerer, P., 1993. The Avalanche Handbook. The Mountaineers, Seattle, WA.
Mears, A., 1992. Snow-avalanches hazard analysis for land-use planning and engineering. Colorado Geological Survey, Department of Natural Resources, Denver, Bulletin 49, 17–19.
MEDD, CEMAGREF, ONF, 2006. Enquête Permanentes sur les Avalanches (EPA), Liste des sites et des événements, commune de la Grave.
Moran, P.A.P., 1950. Notes on continuous stochastic phenomena. Biometrika 37, 17–23.
Mundo, I.A., Barrera, M.D., Roig, F.A., 2007. Testing the utility of *Nothofagus pumilio* for dating a snow avalanche in Tierra del Fuego, Argentina. Dendrochronologia 25, 19–28.
Muntan, E., Andreu, L., Oller, P., Gutiérrez, E., Martinez, P., 2004. Dendrochronological study of the Canal del Roc Roig avalanche path: first results of the Aludex project in the Pyrenees. Annals of Glaciology 38, 173–179.
Muntan, E., Garcia, C., Oller, P., Martí, A., Garcia, A., Gutiérrez, E., 2009. Reconstructing snow avalanches in the Southeastern Pyrenees. Natural Hazards and Earth System Sciences 9, 1599–1612.
Navarre, J.P., Villecrose, J., Pahaut, E., König-Barde, J., 1991. Caractères exceptionnels de l'enneigement du début de l'hiver 1989/90. Neige et Avalanches 53 (54), 15–23.
Ozenda, P., 1985. La végétation de la chaîne alpine dans l'espace montagnard européen. Masson, Paris.
Poggi, A., Plas, J., 1969. Conditions météorologiques critiques pour le déclenchement des avalanches. Symposium on snow avalanches, Davos IAHS Pub, 69, pp. 25–34.
Potter, N., 1969. Tree-ring dating of snow avalanche tracks and the geomorphic activity of avalanches, northern Absaroka Mountains, Wyoming, Boulder, CO. Geological Society of America Special Paper 123, 141–165.

R Development Core Team, 2007. R: a Language and Environment for Statistical Computing. R Foundation for Statistical Computing, Vienna, Austria. http://www.R-project.org.

Rayback, S.A., 1998. A dendrogeomorphological analysis of snow avalanches in the Colorado Front Range, USA. Physical Geography 19, 502–515.

Reardon, B.A., Pederson, G.T., Caruso, C.J., Fagre, D.B., 2008. Spatial reconstructions and comparisons of historic snow avalanche frequency and extent using tree rings in Glacier National Park, Montana, U.S.A. Arctic, Antarctic, and Alpine Research 40, 148–160.

Rinn, F., 2003. TSAP-Win, Software for Tree-Ring Measurement, Analysis and Presentation. Rinntech, Heidelberg.

Ripley, B.D., 1996. Pattern Recognition and Neural Networks. Cambridge University Press, Cambridge.

Schaerer, P.A., 1972. Terrain and vegetation of snow avalanche sites at Rogers Pass, British Columbia in Mountain Geomorphology. In: Slaymaker, O., McPherson, H.J. (Eds.), Tantalus Research Ltd., Vancouver, BC, pp. 215–222.

Schneuwly, D.M., Stoffel, M., Bollschweiler, M., 2009. Formation and spread of callus tissue and tangential rows of resin ducts in *Larix decidua* and *Picea abies* following rockfall impacts. Tree Physiology 29, 281–289.

Schweingruber, F.H., 1996. Tree Rings and Environment. Dendroecology. Paul Haupt, Bern, Stuttgart, Wien.

Shigo, A.L., 1984. Compartimentalization: a conceptual framework for understanding how trees grow and defend themselves. Annual Review of Phytopathology 22, 189–214.

Shroder, J.F., 1978. Dendrogeomorphological analysis of mass movement on Table Cliffs Plateau, Utah. Quaternary Research 9, 168–185.

Stoffel, M., Bollschweiler, M., 2008. Tree-ring analysis in natural hazards research—an overview. Natural Hazards and Earth System Sciences 8, 187–202.

Stoffel, M., Bollschweiler, M., 2009. What tree rings can tell about earth-surface processes. Teaching the principles of dendrogeomorphology. Geography Compass 3, 1013–1037.

Stoffel, M., Hitz, O.M., 2008. Snow avalanche and rockfall impacts leave different anatomical signatures in tree rings of *Larix decidua*. Tree Physiology 28, 1713–1720.

Stoffel, M., Perret, S., 2006. Reconstructing past rockfall activity with tree rings: some methodological considerations. Dendrochronologia 24, 1–15.

Stoffel, M., Schneuwly, D., Bollschweiler, M., Lièvre, I., Delaloye, R., Myint, M., Monbaron, M., 2005. Analyzing rockfall activity (1600–2002) in a protection forest—a case study using dendrogeomorphology. Geomorphology 68, 224–241.

Stoffel, M., Bollschweiler, M., Hassler, G.R., 2006. Differentiating past events on a cone influenced by debris-flow and snow avalanche activity—a dendrogeomorphological approach. Earth Surface Processes and Landforms 31, 1424–1437.

Therneau, T.M., Atkinson, E.J., 1997. An Introduction to Recursive Partioning using the RPART Routines. Technical Report. Mayo Foundation.

Timell, T.E., 1986. Compression Wood in Gymnosperms. Springer-Verlag, Berlin.

Villecrose, J., 2001. Les avalanches de janvier et février 1999 dans les Alpes du Nord françaises; contexte-météorologique et comparaison avec les épisodes passés. La Météorologie 32, 11–22.

Ward, R.G.W., 1985. An estimate of avalanche frequency in Glen Feshie, Scotland, using tree rings. In: Fieller, N.R.J., Gilbertson, D.D., Ralph, N.G.A. (Eds.), Palaeoenvironmental Investigations: Research Design, Methods and Data Analysis: Symposium Number 5 of the Association for Environmental Archaeology, British Archaeological Reports International Series, 258, pp. 237–244.